

Original Research

# Dynamic Monitoring of CD200 Mediated by Ascites-Derived Exosomes as a Predictor of Survival and Response to Front-Line Chemotherapeutics in Advanced High-Grade Serous Ovarian Cancer

Ying Ji<sup>1</sup>, Shanshan Liu<sup>1</sup>, Genju Wang<sup>1</sup>, Xin Chen<sup>1</sup>, Yujuan Li<sup>2</sup>, Xiaogai Zhi<sup>3</sup>,  
Hongxiu Jiang<sup>1</sup>, Juan Tang<sup>1</sup>, Yi Ding<sup>1</sup>, Shuli Zhao<sup>4</sup>, Hongmei Zhou<sup>5</sup>, Aiwei Xiong<sup>1,\*</sup><sup>1</sup>Department of Gynecology and Obstetrics, the Second Hospital of Nanjing, Nanjing University of Chinese Medicine, 210003 Nanjing, Jiangsu, China<sup>2</sup>Department of Gynecology and Obstetrics, Nanjing First Hospital, Nanjing Medical University, 210006 Nanjing, Jiangsu, China<sup>3</sup>Department of Gynecology and Obstetrics, Nanjing Maternal and Child Health Care Hospital, Nanjing Medical University, 210011 Nanjing, Jiangsu, China<sup>4</sup>Department of the Central Lab, Nanjing First Hospital, Nanjing Medical University, 210006 Nanjing, Jiangsu, China<sup>5</sup>Department of Gynecology and Obstetrics, Nanjing Jiangning Hospital, Nanjing Medical University, 211100 Nanjing, Jiangsu, China\*Correspondence: [jiedushi\\_xiong@163.com](mailto:jiedushi_xiong@163.com) (Aiwei Xiong)

Academic Editor: Andrea Tinelli

Submitted: 3 April 2023 Revised: 31 May 2023 Accepted: 5 June 2023 Published: 19 October 2023

## Abstract

**Background:** Exosomes, harboring donor-cell-derived biomarkers, are implicated in transferring oncologic protein and genetic materials. CD200, an immune checkpoint, has been engineered to affect immunosuppression in ovarian cancer. However, the potential of CD200 to serve as a predictor of ovarian cancers remains unexplored. **Methods:** We performed dynamic measurements of exosome-mediated or serum CD200 levels at primary diagnosis, post-operation, and three cycles after chemotherapy. The receiver operating characteristic curve and cumulative survival rate were paralleled to decode the predictive and prognostic profiles. **Results:** Independent enrichment and identification of exosomes revealed a significant concentration of CD200, predominantly located within these exosomes. The CD200 level was elevated in non-responders compared to responders at the serial points and significantly decreased after treatment. At the 335.50 pg/mL cut-off, CD200 at primary diagnosis enabled accurate discrimination between responders and non-responders with an area under the curve (AUC) of 0.94 (95% confidence interval (CI) = 0.902–0.979,  $p = 0.01$ ). With the cut-off dropping from 311.00 pg/mL to 265.00 pg/mL, the AUC decreased from 0.918 (95% CI = 0.873–0.963,  $p = 0.02$ ) to 0.908 (95% CI = 0.862–0.955,  $p = 0.02$ ), respectively. Elevated levels of CD200 levels at both primary diagnosis and three cycles after chemotherapy were identified as independent predictors for poor progression-free survival (PFS) (hazard ratio (HR) = 2.8, 95% CI = 2.08–3.49,  $p = 0.01$ ; HR = 6.7, 95% CI = 4.01–8.02,  $p = 0.01$ , respectively) and overall survival (OS) (HR = 3.5, 95% CI = 2.14–4.99,  $p = 0.04$ ; HR = 5.6, 95% CI = 3.01–7.34,  $p = 0.01$ , respectively). Based on CD200 dynamics, patients were stratified into high- and low-AUC groups. High CD200-AUC was independently associated with unfavourable PFS and OS (HR = 4.6, 95% CI = 3.6–15.7,  $p = 0.01$ ; HR = 3.2, 95% CI = 1.5–6.3,  $p = 0.01$ , respectively). **Conclusions:** This study proposes high exosome-mediated CD200 as a liquid-based biomarker indicative of chemotolerance and dismal survival in ovarian neoplasms.

**Keywords:** exosome; ovarian cancer; CD200; prognosis; response

## 1. Introduction

Advanced high-grade serous ovarian cancer (HG-SOC), the most lethal subtype of gynaecological malignancy, ranks as the seventh most commonly diagnosed tumor among women [1]. Approximately 230,000 cases are recorded and 15,000 deaths are documented, annually [2]. Primary debulking or radical resection, complemented by neoadjuvant or adjuvant therapy such as platinum-based chemotherapeutics, has become a backstone in managing ovarian neoplasms, with widespread adoption and utilization. Despite this, the advanced stage presents a rate of 29% of 5-year survival, in contrast to 92% in the early stage [3]. Patients defined as platinum-resistant, experiencing relapse within six months post-chemotherapy, exhibited a significant decrease in overall survival (OS) of approximately 12

months, as well as dismal progress-free survival (PFS) of about four months [4]. While most HG-SOC occurs in post-menopausal women, 12.1% of those with reproductive fertility are younger than 44 years old [5]. Cryopreservation and the closed verification system represent the established method in the clinical field of fertility [6].

Carrying informative biomarkers in heterogeneous cargos, exosomes comprise growth factors, membrane receptors, and nucleic acids, mirroring the originating cell and modulating tumorigenic pathways [6]. More recently, exosomes have been shown to function in tumor malformation, metastasis [7,8] and especially in chemoresistance [9–11]. For instance, Battke *et al.* [12,13] reported that tumor cell-derived exosomes could confer drug resistance through immune cell regulation by interaction with TGF $\beta$ 1 and PDL-1; Nabet Barzin Y *et al.* [14] proved that unshielded RN7SL1,



mediated by exosome, exasperated drug resistance by binding and activating retinoic acid-inducible gene I.

A range of biomarkers has been decoded to facilitate therapy monitoring and predict prognosis. However, none of them bore fruit when exploited in clinical routine. CD200, formerly termed OX-2, a highly conserved transmembrane glycoprotein, was previously targeted as an immune checkpoint. Together with its receptors CD200R1-R4, CD200 is predominantly located in endothelial cells, neurons, and T and B lymphocytes [15]. The interaction of CD200 and receptors facilitates the downstream of immunosuppressive pathways, leading to the repression of regulator T cells [16], the switch of cytokine from Th1 to Th2 [17] and peripheral tolerance [18]. Siva *et al.* [19] reported that strong stained CD200 might permit a highlighted anti-tumor response when blocked with an antagonistic antibody in ovarian tumors. Chen *et al.* [20] identified CD200 as an anti-inflammatory mediator, preventing ovarian hyperstimulation syndrome by maintaining the vascular barrier. However, the predictive or prognostic role of CD200 in HGSOE remains unexplored.

In this study, we attempted to unravel the predictive and prognostic role of CD200 by dynamically monitoring the lineage change from the onset of surgery to the completion of chemotherapy. We interrogated: (i) whether CD200 would be overexpressed in exosomes or serum; (ii) whether CD200 could predict response and survival.

## 2. Methods

### 2.1 Patients, Ethics and Eligible Criteria

This project was predominantly conducted at the Department of Gynaecology and Obstetrics in Nanjing Second Hospital. 175 primary documented ovarian cancers were consecutively included from January 2015 to March 2017. All patients provided written informed consent before participation. Eligibility criteria were biopsy-proven HGSOE, International Federation of Gynecology and Obstetrics (FIGO) stage III or IV, debulking resection followed by front-line platinum-based adjuvant chemotherapy, and presence of both ascites and serum samples for analysis. Exclusion criteria were at least 20% sample points not available across the treatment, neoadjuvant chemotherapy, uncontrollability of diabetes mellitus or hypertension, chemotherapy contraindications (infection, intestinal ileus), and secondary malignancies. All included cases experienced the primary tumor debulking aiming at macroscopic clearance, followed by first-line platinum-based chemotherapeutics. Bevacizumab was consecutively delivered, particularly in patients with at least FIGO IIIb, regardless of platinum sensitivity or resistance.

### 2.2 Definition and Sample Size Calculation

OS was defined as the interval from surgical intervention to death or the last follow-up. PFS was calculated from the onset of surgery until the date of relapse, including lo-

cal recurrence or distant metastasis. Platinum-free interval (PFI) was the time elapsed from the last platinum dose until clinical recurrence, defining platinum-sensitivity/responder (PFI >6 months) and platinum-resistance/non-responder (PFI ≤6 months). Cases were censored if still alive at analysis or died from other causes. Tumor was graded in agreement with the Surgical Pathological Classification revised in 2013 by the FIGO. Sample size was calculated based on 0.80 sensitivity, 0.80 specificity, 0.05 type I error, 0.10 tolerance error, and 0.20 type II error estimates. Authors cannot access information that could identify individual participants during or after data collection.

### 2.3 Exosome Isolation

Ascites were withdrawn through transabdominal tubes, immediately rotary mixed, and transferred into sterile centrifuge tubes. Within 1 hour after withdrawal, the floating cells were removed by centrifugation at 300 ×g spin for 10 minutes using Optima XPN XE-90 (Beckman Coulter Inc., Brea, CA, USA). Dead cells deposited at the bottom were cleared at 2500 ×g for 10 minutes. According to the outlined protocol, exosomes were extracted through the mixture of supernatants with a 1.0 mL volume of Total Exosome Isolation Reagent (cat. no.4484453, Invitrogen Inc., Carlsbad, CA, USA) by repeatedly pipetting before the specimens turned homogenous. The upper compound exosomes were centrifuged at 10,000 ×g for 30 minutes, re-suspended, and then centrifuged at 100,000 ×g for 70 minutes. Finally, the purified exosomes redissolved in 100 μL phosphate-buffered solution (cat. no. P4414, Sigma, St. Louis, MO, USA) were divided into sterile Eppendorf tubes stored at -80 °C for further processing. Samples were blinded to enable conditions of processing undiscovered. Freeze-thaw was avoided throughout the procedure.

### 2.4 Electron Microscopy

Sodium cacodylate buffer was used to wash exosomes at pH 7.35–7.45, after which 3% osmium tetroxide was applied for post-fixation. Exosomes were dehydrated using a propylene oxide wash for 5 minutes and rinsed with ethanol again, followed by incubation in propylene oxide for up to 24 hours in 60 °C incubators. A mixture of propylene oxide was administered to embed the specific exosome pellets at 60 °C for one night. 80 nm sections were cut using ultramicrotome RM2235 (Leica GmbH, Wetzlar, Germany) and contrasted with 4% uranylacetate and Sato's stain. Transmission electron microscope JEM-1010 (JEOL, Akisima, Tokyo, Japan) was performed to capture the samples at 80 kV.

### 2.5 Quantitative Real-Time Polymerase Chain Reaction (PCR)

The total RNA was extracted from 100 μL purified exosomes or ascites samples employing Reagent™ (Invitrogen, Carlsbad city, CA, USA) in accordance with the proto-

**Table 1. The relation between baseline characteristics and treatment response.**

		Non-responder n = 57 (%)	Responder n = 91 (%)	<i>p</i>	Logistic regression	
					95% CI	<i>p</i>
Age (years)		52.3 ± 12.2	51.6 ± 12.0	0.76	0.92–1.03	0.60
Menopause	Yes	32 (56.1)	52 (57.1)	0.905	0.37–4.38	0.70
	No	25 (43.9)	39 (42.9)			
FIGO (2013)	III	25 (43.9)	37 (40.6)	0.701	0.09–1.92	0.267
	IV	32 (56.1)	54 (59.4)			
Macroscopic residual	Yes	35 (61.4)	54 (59.3)	0.803	0.50–10.4	0.28
	No	22 (38.6)	37 (40.7)			
<i>BRCAl/2</i> mutation	Mutated	16 (28.1)	28 (30.8)	0.727	0.54–2.43	0.71
	Not yet	41 (71.9)	63 (69.2)			
HRD status	Positive	20 (35.1)	35 (38.5)	0.827	0.55–3.10	0.65
	Negative	37 (64.9)	56 (61.5)			
Bevacizumab administration	Yes	11 (19.3)	15 (16.5)	0.70	0.34–4.35	0.65
	No	46 (80.7)	76 (83.5)			
TC cycles		4.9 ± 1.6	5.1 ± 1.9	0.51	0.80–1.45	0.48
CA125 (U/mL)		2545 ± 650	2704 ± 785	0.20	0.13–1.34	0.25

Data presented as mean ± standard deviation or n (%).

FIGO, International Federation of Gynecology and Obstetrics; HRD, homologous recombination deficiency; TC, taxol and carboplatin; CI, confidence interval.

col. cDNA was produced using the TaqMan Reverse Transcription Kit (Thermo Fisher, Waltham, MA, USA). Ultimately, a 20 µL volume was prepared using Taqase (2 µL), dNTP (2 µL), RNasin (1 µL), SYBN Marker (1 µL), and primers (2–4 µL). On Applied Biosystems 7500 (Thermo Fisher, Waltham, MA, USA), the cultivated reagent was subjected to SYBR green-based real-time polymerase chain reaction (RT-PCR). Each sample point was determined in triplicate, with PBS as the negative control. The data were retrieved and displayed by comparison using the  $2^{-\Delta\Delta C_t}$  method [21]. During the thermal cycling, 95 °C was maintained for 30 s, followed by 40 cycles of 5 s at 95 °C and 30 s at 60 °C. Custom-designed primers:  $\beta$ -actin, Forward-AGA AAA TCT GGC ACC ACA CC, Reverse-CCA TCT CTT GCT CGA AGT CC; ALIX, Forward-GAC GCT CCT GAG ATA TTA TGA TCA GA, Reverse-ACA CAC AGC TCT TTT CAT ATC CTA AGC; CD60, Forward-GAA TTC TGC GCC CTC GGT T, Reverse-CTG CCT CAG TCC GGG AGA TA.

### 2.6 Enzyme-Linked Immunoabsorbent Assay

The concentrations of CD200 in ascites, purified exosomes and serum were quantified using the commercially available CD200 enzyme-linked immunoabsorbent assay kit (catalog: P41217, Wuhan Enfei Biotechnology, Wuhan, Hubei, China). After equilibration at 20–25 °C, the samples and reagents were incubated at 37 °C for 90 minutes. In the standard diluent buffer, samples (2 × 10 µL) were diluted in 1:5. The prepared samples were analyzed in duplicate. Based on the double-antibody sandwich assay, 75 pg/mL specificity was achieved. Optical densities were measured at 450 nm by the NOVA 60A Spectroquant pho-

tometer (Merck KGAA, Darmstadt, Germany). The CD200 level was interpolated from the standard curve using a logistic fit with four parameters, with the low and high detection limits being 25 and 8000 pg/mL, respectively.

### 2.7 Statistic Analysis

Chi-squared and Student's *t*-tests were employed to discriminate the descriptive parameters. Mann-Whitney U was performed for testing CD200 homogeneity between groups, and Wilcoxon rank-sum for CD200 dynamics within groups. The receiver operating characteristic curve (ROC) was plotted, and the area under the curve (AUC) was calculated. At the maximum of the Youden index, the optimal cut-off was determined. The Kaplan-Meier curve was constructed to parallel the cumulative rate of OS to PFS using the Log-rank test. Univariable and multivariable Cox proportional regressions were modeled. A hazard ratio (HR) and 95% confidence interval (CI) were indicated. SPSS version 26 (SPSS Inc., Chicago, IL, USA) and GraphPad Prism 8 (GraphPad Software, LaJolla, CA, USA) were developed for analysis and presentation. Two-tailed  $p < 0.05$  was considered significant.

## 3. Results

From January 2015 to March 2017, 175 patients were enrolled at the Department of Gynaecology and Obstetrics in the Nanjing Second Hospital. Twelve patients withdrew written informed consent, and 15 cases declined before the project launch. Missing data (61/444, <15%) across the treatment were covered with multiple interpolations. The baseline characteristics are summarized in Table 1. The average age of non-responders was 52.3 + 12.2 years, while

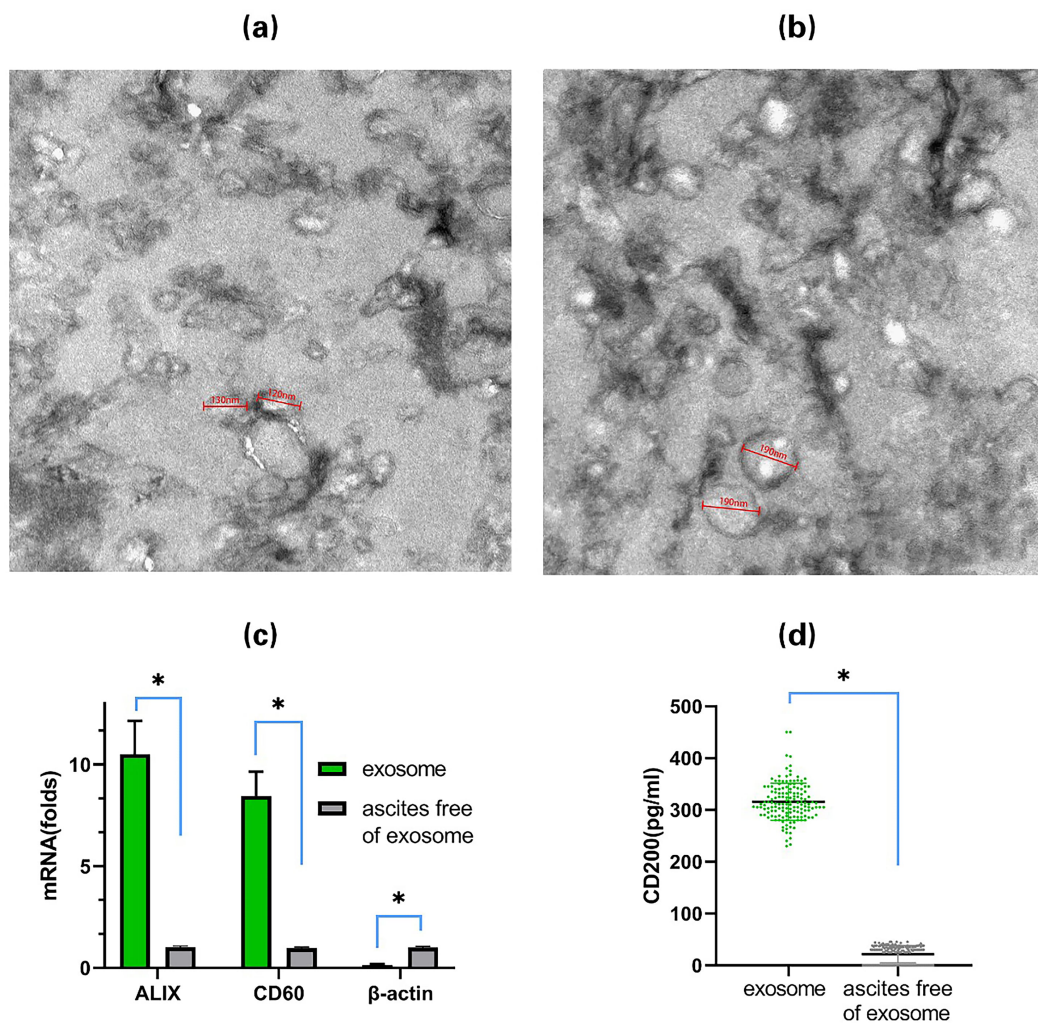


**Fig. 1. Isolation and characterization of exosome drawn from ascites.** Electron microscopy identifying exosome isolated from responder (a) and non-responder (b) at 80 kv. Vehicles are displayed between 40–190 nm in diameter. Real-time PCR validating highly enriched exosome colony (c) based on common exosome markers, including ALIX, CD60 and the absence of  $\beta$ -actin. Enzyme-linked immunoabsorbent assay comparing CD200 expression in exosome and ascites free of exosome groups (d). \*,  $p < 0.05$ . PCR, polymerase chain reaction.

respondent group was  $51.6 \pm 12.0$  years. The majority of HGSOc experienced the macroscopic residual. Up to 30% of patients carried mutated *BRCA1/2* genes, and approximately 40% harbored a positive homologous recombination deficiency (HRD) status.

### 3.1 Exosomes were Enriched and CD200 was Mainly Located in Exosomes

We isolated the exosomes at super speed and identified those specific particles utilizing a Transmission electron microscope. In Fig. 1a (responder) and Fig. 1b (non-responder), exosomes were displayed between 30–170 nm in diameter. Validated by real-time PCR, those vehicles were highly enriched based on the expression of exosome biomarkers ALIX, CD60 and the absence of  $\beta$ -actin ( $p < 0.05$ ,  $p < 0.05$ ,  $p < 0.05$ , respectively; Fig. 1c). CD200 expression in exosomes was  $315.4$  ( $290$ – $340$ ) pg/mL, as com-

pared to  $21.5$  ( $0$ – $35$ ) pg/mL in ascites free of exosomes ( $p < 0.001$ , Fig. 1d).

### 3.2 CD200 was Elevated in Non-Responders and Declined in the Treatment Course

We detected CD200 levels in HGSOc at primary diagnosis, post-operation and three cycles after chemotherapy (Fig. 2). CD200 appeared to be predominantly located in serous ovarian cancer (Fig. 2a). In serum or ascites without exosome, CD200 was scarcely observed, with levels holding stable across treatment (Fig. 2b,d). A linear correlation test proposed a weak linear relation between serum CA125 and exosome-mediated CD200 ( $R^2 = 0.038$ ,  $p < 0.05$ ; Fig. 2e). In the exosome of total HGSOc cases, CD200 was highly enriched and rapidly decreased after surgery and adjuvant chemotherapy (Fig. 2c). Compared to responders, the CD200 level in non-responders was highly

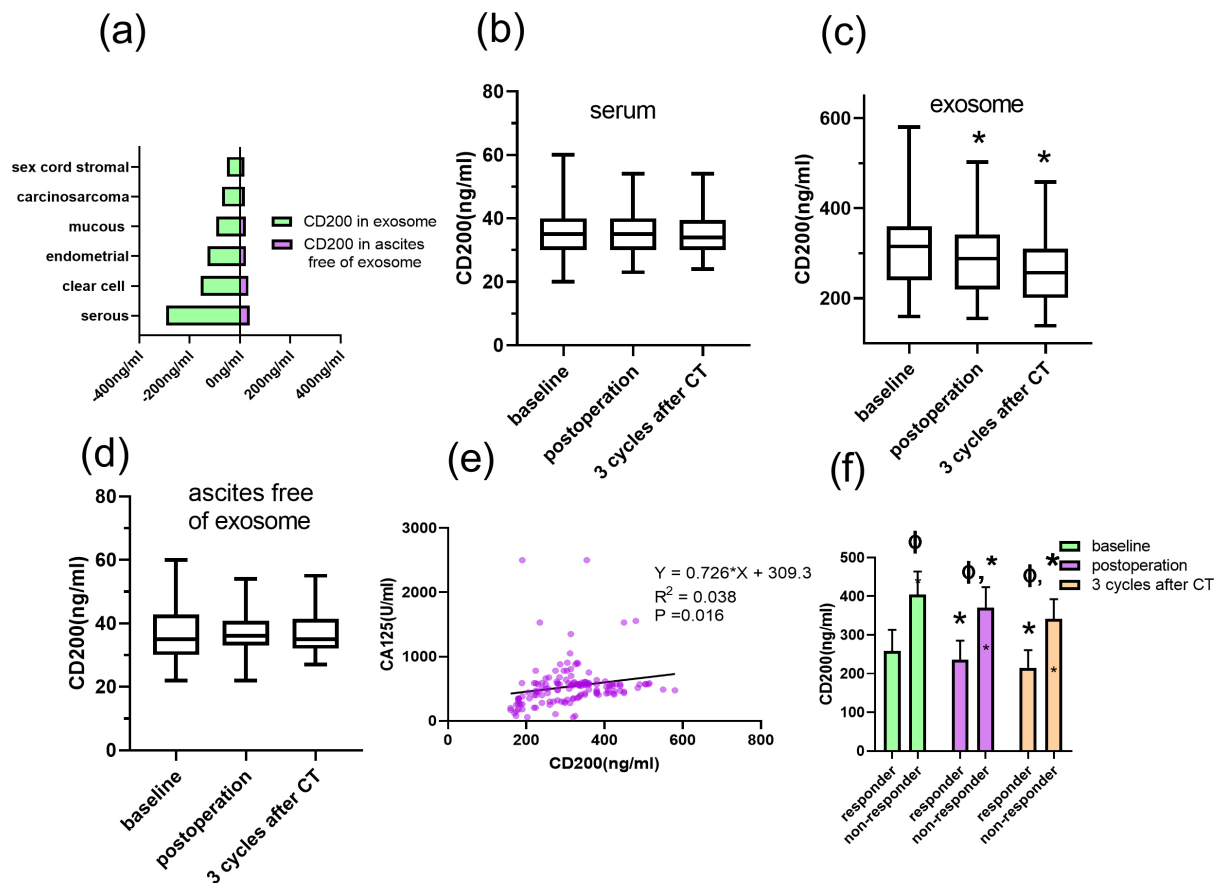


**Fig. 2. Dynamic CD200 levels across surgery and adjuvant platinum-based therapy.** The CD200 level was compared in various histologies (a). The CD200 in serum (b), exosome (c) and ascites free of exosome (d) was detected at primary diagnosis, as well as after radical resection (post-operation) and three cycles after chemotherapy (post-3 cycles). The linear correlation between CA125 and CD200 was examined (e). CD200 concentration was predominantly detected in responders and non-responders (f). A *p*-value is calculated using the Maan-Whitney U test for independent samples and the Wilcoxon rank sum test for paired samples. \*, *p* < 0.05 compared to the previous level within groups;  $\phi$ , *p* < 0.05 compared to the responder group at corresponding points. The Spearman test was conducted for a linear correlation, and  $R^2$  or linear equation was indicated. CT, chemotherapy.

elevated at first diagnosis as well as the following points (all *p* < 0.001), declining after primary surgery and adjuvant chemotherapy (all *p* < 0.001, Fig. 2f).

### 3.3 CD200 could Accurately Discriminate Responders from Non-Responders

ROC analysis showed that CD200 at the primary diagnosis enabled robust discrimination between responders and non-responders with an AUC of 0.94 (95% CI = 0.902–0.979, *p* = 0.01). Responders were detectable from the total cohort at 335.50 pg/mL, exhibiting a sensitivity of 0.842 and specificity of 0.92 (Fig. 3a); as the cut-off dropped to 311.00 pg/mL, the discriminative power decreased to 0.918 (95% CI = 0.873–0.963, *p* = 0.02), representing a sensitivity of 0.78 and a specificity of 0.89 (Fig. 3b); with 265.00 pg/mL as a cut-off after completion of 3-cycle chemotherapy, the AUC declined to 0.908 (95% CI = 0.862–0.955, *p* = 0.02), resulting in a sensitivity of 0.89 and specificity of 0.77. (Fig. 3c)

### 3.4 High CD200 could Predict Poor Survival in Ovarian Cancers

Stratified by CD200, the median PFS of the high group was 5.1 months, which was shorter than the low group at primary diagnosis (8.6 months, 95% CI = 2.8–9.7, *p* = 0.001, Fig. 4a). Similarly, the median PFS of the high CD200 group significantly declined compared to the low CD200 group at post-operative and post-3 cycles ( 4.9 vs. 8.7 months, 95% CI = 2.2–6.1, *p* < 0.001, Fig. 4b; 5.8 vs. 10.1 months, 95% CI = 2.4–8.1, *p* < 0.001, Fig. 4c, respectively ). Multivariate regression analysis revealed that a high CD200 at primary and post-3 cycles facilitated poor PFS, independently from established risk factors (HR = 2.8, 95% CI = 2.08–3.49, *p* = 0.01; HR = 6.7, 95% CI = 4.01–8.02, *p* = 0.01, respectively, Table 2). The median OS for the high CD200 group was 10.4 months, poorer than 19.8 months in low group at primary diagnosis (95% CI = 2.2–7.6, *p* < 0.001, Fig. 4d). Similarly, the high CD200 group

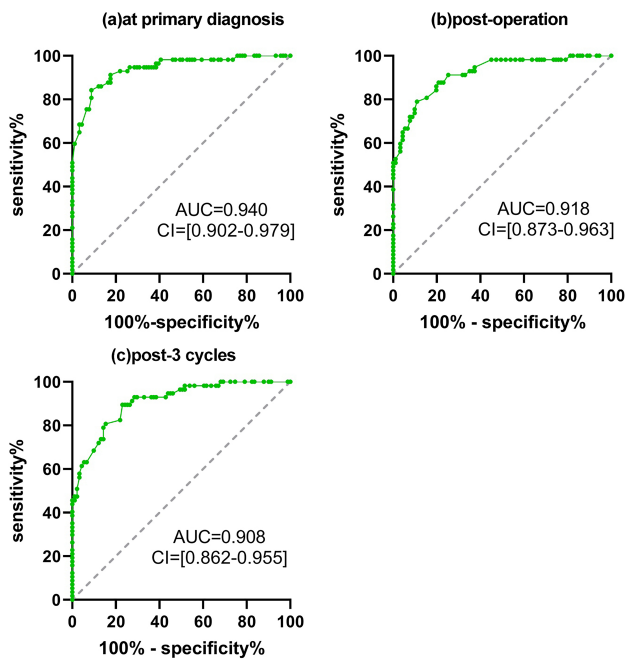


**Fig. 3. Receiver operating characteristic curve (ROC) of CD200 across surgery and adjuvant platinum-based therapy.**

For the serial threshold of CD200, the true positivity against false positivity was generated between responders and non-responders at primary diagnosis (a), post-operation (b) and post-3 cycles of chemotherapy (c). The area under the curve (AUC) and 95% confidence interval (CI) are indicated.

exhibited a lower OS compared to the low CD200 group at post-operation and three cycles after chemotherapy (10.5 vs. 20.5 months, 95% CI = 2.5–8.1,  $p < 0.001$ , Fig. 4e; 12.5 months vs. 23.6 months, 95% CI = 1.9–5.2,  $p < 0.001$ , Fig. 4f, respectively). In Cox proportional regression, high CD200 at primary and post-3 cycles independently correlated with poor OS (HR = 3.5, 95% CI = 2.14–4.99,  $p = 0.04$ ; HR = 5.6, 95% CI = 3.01–7.34,  $p = 0.01$ , respectively, Table 3). Further, we tracked CD200 lineage and dynamics throughout treatment by interconnecting serial CD200 values. As compared to the low CD200-AUC group, the PFS and OS of the high CD200-AUC group were significantly reduced (5.2 vs. 9.3 months, 95% CI = 2.2–6.4,  $p < 0.001$ ; 12.0 vs. 20.5 months, 95% CI = 1.9–5.6,  $p < 0.001$ , respectively, Fig. 5). Cox proportional regression revealed that high CD200-AUC was independently corrected with poor PFS and OS (HR = 4.6, 95% CI = 3.6–15.7,  $p = 0.01$ , Table 2; HR = 3.2, 95% CI = 1.5–6.3,  $p = 0.01$ , Table 3, respectively).

## 4. Discussion

Contrary to circulating biomarkers, ascites molecule profiles are more likely stable as they are less susceptible to vascular endothelial infiltration or organ metabolism changes. In this context, extracting CD200 from ascites di-

rectly reflects the tumor's biogenesis and could enhance its potential to customize treatment intensity and duration. Using a serial sampling approach, we demonstrated three critical utilities in patients harboring HGSOc: the CD200 is highly expressed in non-responders' ascites; CD200 accurately predicts response to platinum-based chemotherapeutics after curative intent surgery; increased CD200 correlates with impaired PFS and OS in point or lineage dynamic settings. These encouraging results represent the first data indicating the potential of CD200 as a suitable marker for predicting response or prognosis in solid tumors.

Versatile mechanisms have been established to prevent tumors from being sensitized to antineoplastic drugs, including increased drug efflux, frequent DNA damage repair, and strengthened ability to undergo epithelial-to-mesenchymal transition. Studies have recognized that bioengineered exosomes could facilitate the packing and transportation of anti-cancer treatments out of the tumor microenvironment. This process may contribute to developing acquired resistance to targeted drugs [22]. We found that CD200 mediated by exosomes was highly expressed in the ascites of non-responders, indicating that CD200 is engaged in counteracting the platinum effect in HGSOc patients after primary surgery. CD200 delivered in nanosized cargos might detoxify drugs by inactivating the expression of Mcl-1 and surviving [23]. In Yuh-Seog Jung's study [24], activating Bmi-1 and SHH in CD200-overexpressing squamous cell carcinomas also imparted a resistance phenotype against chemoradiation. Interestingly, CD200 expression was scarcely observed in ascites without exosomes, possibly because exosomes package predominantly hydrophobic and soluble CD200, thus allowing unique CD200 delivery for intercellular cross-talk. Siva *et al.* [19] confirmed the membrane-associated CD200 staining by immunohistochemistry in ovarian cancer. However, there has been no serum CD200 analysis in HGSOc. In our study, we proposed that CD200 is minimally present in the serum; we found that serum-based CD200 is not applicable for dynamic detection due to the stable expression. It is notable and puzzling that CD200 is highly enriched in ascites, especially in exosomes, but little in serum. The limited diffusion of CD200 into the circulating system may be attributed to the unique membrane budding and endosomal sorting machinery of exomes [22,25,26]. These mechanisms likely restrict the release of CD200 into the bloodstream. The membrane-bundled CD200 is persistently secreted into ascites, which could compete with the endothelium filtration of blood and lymphatic vessels.

With *BRCA1/2* gene mutation and HRD status included in the final analysis, we could somewhat weaken the heterogeneous bias, which might be associated with chemosensitivity. In regard to response prediction, the persistently detectable CD200 provided excellent discrimination between responders and non-responders at primary diagnosis, post-operation, and following three cycles of

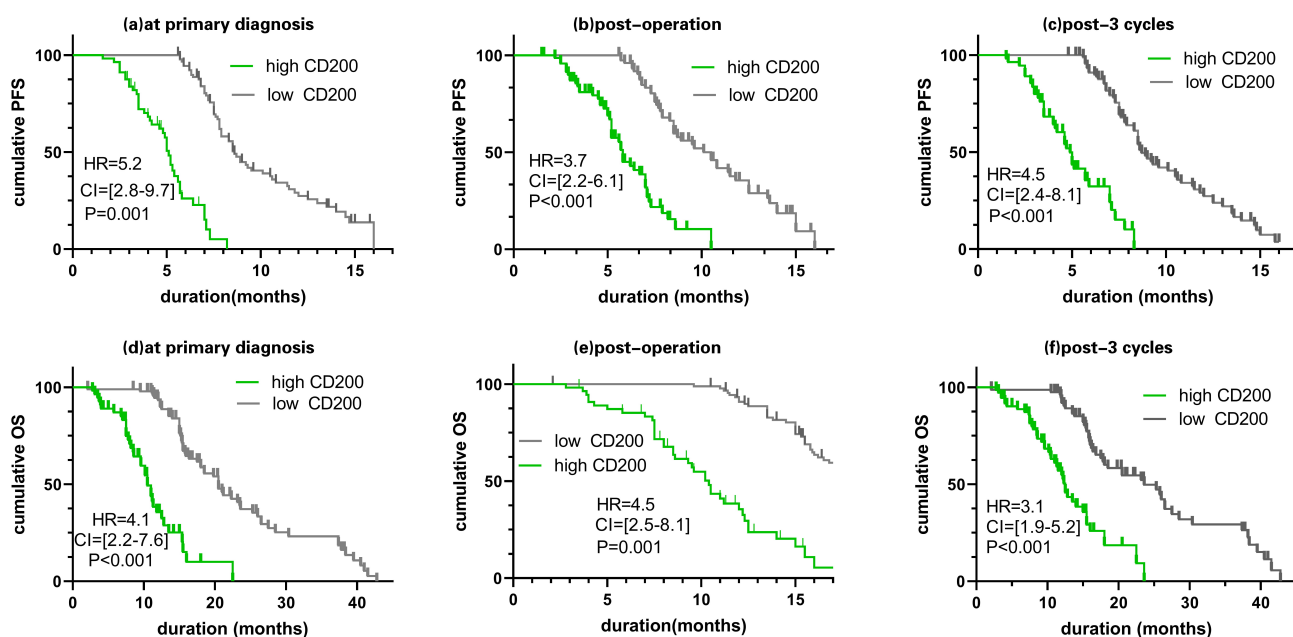


**Fig. 4. Prognostic discrepancy across radical resection and adjuvant chemotherapy based on CD200 levels.** Kaplan-Meier comparing progression-free survival (PFS) and overall survival (OS) in individuals with high CD200 level versus low CD200 level at primary diagnosis (a,d), post-operation (b,e) and post-3 cycles (c,f). The cutoff value stratifying CD200 levels into high and low levels was estimated by maximizing the Youden index. *p*-value, 95% confidence interval (CI) and hazard ratio (HR) are indicated.

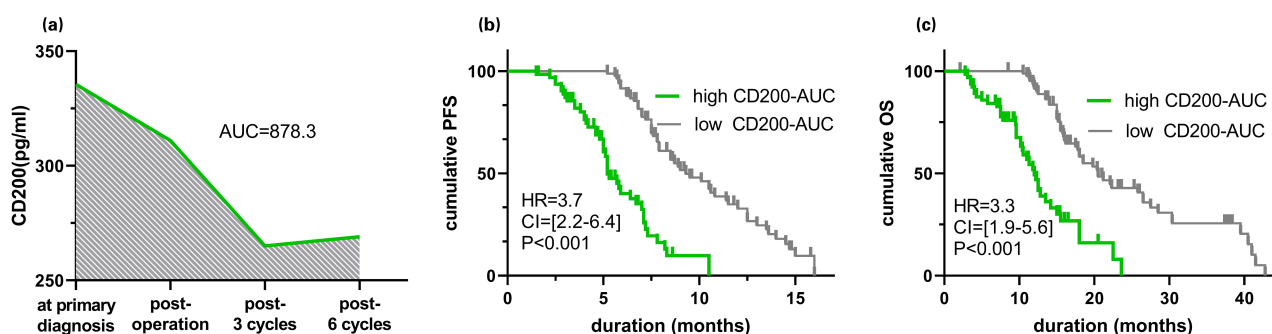


**Fig. 5. Prognostic discrepancy across radical resection and complementary chemotherapy based on CD200-AUCs.** CD200 linear dynamics between the primary diagnosis and 6 chemotherapy cycles (a). The cutoff value was determined by maximizing the Youden index for stratifying the studies into low and high CD200-AUC groups. The Kaplan-Meier curve was generated to analyze (b) progression-free survival (PFS) and (c) overall survival (OS). A Log-Rank test was calculated. *p*-value, 95% confidence interval (CI), and hazard ratio (HR) are indicated. AUC, area under the curve.

chemotherapy, thus providing a novel surrogate for patients with HGSOE undergoing curative surgery and adjuvant chemotherapy. The strength was superior to that reported in the study by D’Arena *et al.* [27], where circulating CD200 attenuation appears to mount a response to chemioimmunotherapy in chronic lymphocytic leukaemia using 1281 pg/mL as the cut-off point. The rationale may be attributable to the special sprouting and delivery of cross-talk transfectors, directly transmitting the tumorigenesis and inducing immune deficiency related to multidrug resistance. The CD200-screened patients at high risk of platinum resistance should encounter a shift to administering beva-

cizumab, liposomal doxorubicin, and gemcitabine, which the Food and Drug Administration (FDA) approves. In addition, a bevacizumab patient should be monitored for adverse events, such as intestinal fistulas, albuminuria, and hypertension.

To establish the validity of this marker, we enrolled a cohort of high-grade, serous and advanced patients to assess their response to platinum-based chemotherapeutics. This approach aimed to shed light on the predictive value of CD200 in this specific patient population. In this study, we optimized the prognosis stratification based on the same cut-off point determined in the ROC curve at longitude set-

**Table 2. Cox proportional hazards regression associated with PFS.**

	PFS					
	Univariable COX			Multivariable COX		
	HR	95% CI	<i>p</i>	HR	95% CI	<i>p</i>
FIGO (2013)	2.7	2.1–6.6	<0.01	3.5	2.4–11.1	<0.01
Bevacizumab administration	0.3	0.2–0.7	<0.01	0.5	0.1–0.8	<0.01
Macroscopic residual	4.2	2.3–10.7	<0.01	4.8	2.7–13.4	<0.01
<i>BRCA1/2</i> mutation	0.4	0.3–0.8	0.02	0.6	0.4–0.9	0.03
HRD status	0.4	0.1–0.7	0.03	0.3	0.2–0.6	0.04
CD200 at primary diagnosis	2.4	2.35–3.70	0.02*	2.8	2.08–3.49	0.01*
CD200 post-operation	1.8	0.7–5.5	0.19	1.6	0.8–4.6	0.14
CD200 post-3 cycles	5.0	3.05–7.00	0.01*	6.7	4.01–8.02	0.01*
CD200-AUC	4.1	3.3–13.5	0.01*	4.6	3.6–15.7	0.01*

PFS, progression-free survival; FIGO, International Federation of Gynecology and Obstetrics; HRD, homologous recombination deficiency; HR, hazard ratio.

\*,  $p < 0.05$ .

**Table 3. Cox proportional hazards regression associated with OS.**

	OS					
	Univariable COX			Multivariable COX		
	HR	95% CI	<i>p</i>	HR	95% CI	<i>p</i>
FIGO (2013)	2.5	2.1–8.5	0.02	2.6	1.8–9.6	<0.01
Bevacizumab administration	0.3	0.1–0.7	<0.01	0.7	0.2–0.9	0.02
Macroscopic residual	3.3	1.7–9.6	0.02	2.3	1.5–10.4	<0.01
<i>BRCA1/2</i> mutation	0.4	0.3–0.9	0.04	0.8	0.7–0.9	0.04
HRD status	0.2	0.1–0.4	0.03	0.6	0.5–0.8	0.03
CD200 at primary diagnosis	2.2	1.55–3.05	0.01*	3.5	2.14–4.99	0.04*
CD200 post-operation	1.3	0.6–4.0	0.22	1.5	0.62–4.00	0.33
CD200 post-3 cycles	6.1	4.45–10.20	0.01*	5.6	3.01–7.34	0.01*
CD200-AUC	5.5	3.9–16.5	0.01*	3.2	1.5–6.3	0.01*

OS, overall survival; FIGO, International Federation of Gynecology and Obstetrics; HRD, homologous recombination deficiency; HR, hazard ratio.

\*,  $p < 0.05$ .

tings. Among patients receiving three cycles of chemotherapy after surgery, high CD200 levels could enhance the reduced PFS or OS and act as an independent prognosticator after adjusting for known clinicopathological factors. Despite similar risk factors, prognosis could still vary depending on macroscopical residuals, HRD status and *BRCA1/2* gene mutation [28–30]. Alternatively, we speculate that the poor PFS and OS may be attributed to the dysregulation of the tumor microenvironment and the inactivation of tumor-specific T cells induced by CD200 [31]. Compared to tissue biopsy, the CD200 is less invasive and repeatedly detectable. We then determined the AUC by drawing the dynamic lineage curve, which could be additionally used for prediction. The low CD200-AUC group showed a more prolonged PFS and OS than the high CD200-AUC group (9.3 vs. 5.2 months; 20.5 vs. 12.0 months, respectively). Accordingly, the impact of CD200 accumulation across the treatment course, to our speculation, may be dose-dependent and indicate a second-line regimen or a

druggable target. It is worth noting that a second study used tumor stage, optimal debulking, and various serum proteins to predict PFS and identify recurrence in patients with HGSOC [32]. However, our data indicate that even without the clinical-pathological variables, the multivariable Cox proportional regression yields a conclusive result based on liquid-based biomarkers.

While this study presents several advantages as mentioned above, it has certain limitations. First, in FIGO I and II HGSOC patients, the tumor is localized inward of the ovarian membrane, thereby restricting the release of exomes. Moreover, according to clinical practice, illustrating ascites can be challenging, especially in patients with little amount of pelvic ascites. Second, statistical power is generated by assessing the primary endpoint, namely chemotherapeutic response, rather than prognosis, which may attenuate CD200's ability to detect survival discrepancies. Finally, kinetics and clearance of HE4 and CA125 have been reported by some literature as prognostic factors in HG-

SOC [33,34]. Further analysis comparing CD200 with established biomarkers such as CA125 and HE4 in predicting HGSOE should be encouraged.

CD200 mediated by exosomes is up-regulated in non-responders in HGSOE. Dynamic monitoring of CD200 could accurately predict response to chemotherapeutics, especially at primary diagnosis, postoperatively, and following three cycles of chemotherapy. Furthermore, the overexpression of CD200 and a high CD200-AUC indicate poor survival. Noninvasive molecular profiling analysis can potentially guide rational and personalized adjuvant chemotherapy in HGSOE patients following curative intent surgery.

## 5. Conclusions

The CD200 mediated by ascites-derived exosome is up-regulated in advanced HGSOE and indicates dismal PFS and OS, representing an innovative biomarker for predicting HGSOE.

## Availability of Data and Materials

Data not included in this published article or raw data of the manuscript are available upon reasonable request.

## Author Contributions

YJ conceived the idea, performed the procedure and drafted the article. SSL, GJW and XC helped in collecting patient records. YJL organized medical records and interpreted the data. XGZ, YD and HMZ collected and retrieved data. JT helped to design the study and perform the statistical analysis. HXJ supervised the study, reviewed the manuscript and involved in the acquisition and analysis of data. SLZ and AWX coordinated the research and proof-read the manuscript. All authors contributed to editorial changes in the manuscript. All authors have participated sufficiently in the work and agreed to be accountable for all aspects of the work. All authors read and approved the final manuscript.

## Ethics Approval and Consent to Participate

All subjects gave their informed consent for inclusion prior to participating. This study was conducted following the institutional guidelines of the 1964 Helsinki Declaration and its amendments. The study was approved by the Ethics Committee of Nanjing Second Hospital (LS-ky029).

## Acknowledgment

We thank Kaihua Wu for supporting visualization and Minmin Yu for statistics help. We would also like to thank all the obstetrics and gynecology staff at Nanjing Second Hospital, Nanjing University of Chinese Medicine.

## Funding

This research received no external funding.

## Conflict of Interest

The authors declare no conflict of interest.

## References

- [1] Doherty JA, Peres LC, Wang C, Way GP, Greene CS, Schildkraut JM. Challenges and Opportunities in Studying the Epidemiology of Ovarian Cancer Subtypes. *Current Epidemiology Reports*. 2017; 4: 211–220.
- [2] Ferlay J, Soerjomataram I, Dikshit R, Eser S, Mathers C, Rebelo M, *et al.* Cancer incidence and mortality worldwide: sources, methods and major patterns in GLOBOCAN 2012. *International Journal of Cancer*. 2015; 136: E359–E386.
- [3] Reid BM, Permuth JB, Sellers TA. Epidemiology of ovarian cancer: a review. *Cancer Biology & Medicine*. 2017; 14: 9–32.
- [4] Naumann RW, Coleman RL. Management strategies for recurrent platinum-resistant ovarian cancer. *Drugs*. 2011; 71: 1397–1412.
- [5] Kim SY, Lee JR. Fertility preservation option in young women with ovarian cancer. *Future Oncology*. 2016; 12: 1695–1698.
- [6] Gullo G, Perino A, Cucinella G. Open vs. closed vitrification system: which one is safer? *European Review for Medical and Pharmacological Sciences*. 2022; 26: 1065–1067.
- [7] Zhang HG, Grizzle WE. Exosomes: a novel pathway of local and distant intercellular communication that facilitates the growth and metastasis of neoplastic lesions. *The American Journal of Pathology*. 2014; 184: 28–41.
- [8] Azmi AS, Bao B, Sarkar FH. Exosomes in cancer development, metastasis, and drug resistance: a comprehensive review. *Cancer and Metastasis Reviews*. 2013; 32: 623–642.
- [9] Safaei R, Larson BJ, Cheng TC, Gibson MA, Otani S, Naerdmann W, *et al.* Abnormal lysosomal trafficking and enhanced exosomal export of cisplatin in drug-resistant human ovarian carcinoma cells. *Molecular Cancer Therapeutics*. 2005; 4: 1595–1604.
- [10] Shedden K, Xie XT, Chandaroy P, Chang YT, Rosania GR. Expulsion of small molecules in vesicles shed by cancer cells: association with gene expression and chemosensitivity profiles. *Cancer Research*. 2003; 63: 4331–4337.
- [11] Santos JC, Lima NDS, Sarian LO, Matheu A, Ribeiro ML, Derchain SFM. Exosome-mediated breast cancer chemoresistance via miR-155 transfer. *Scientific Reports*. 2018; 8: 829.
- [12] Battke C, Ruiss R, Welsch U, Wimberger P, Lang S, Jochum S, *et al.* Tumor exosomes inhibit binding of tumor-reactive antibodies to tumor cells and reduce ADCC. *Cancer Immunology, Immunotherapy*. 2011; 60: 639–648.
- [13] Martinez VG, O'Neill S, Salimu J, Breslin S, Clayton A, Crown J, *et al.* Resistance to HER2-targeted anti-cancer drugs is associated with immune evasion in cancer cells and their derived extracellular vesicles. *Oncoimmunology*. 2017; 6: e1362530.
- [14] Nabet BY, Qiu Y, Shabason JE, Wu TJ, Yoon T, Kim BC, *et al.* Exosome RNA Unshielding Couples Stromal Activation to Pattern Recognition Receptor Signaling in Cancer. *Cell*. 2017; 170: 352–366.e13.
- [15] Wright GJ, Jones M, Puklavec MJ, Brown MH, Barclay AN. The unusual distribution of the neuronal/lymphoid cell surface CD200 (OX2) glycoprotein is conserved in humans. *Immunology*. 2001; 102: 173–179.
- [16] Gorczynski RM. CD200 and its receptors as targets for immunoregulation. *Current Opinion in Investigational Drugs (London, England: 2000)*. 2005; 6: 483–488.
- [17] Gorczynski L, Chen Z, Hu J, Kai Y, Lei J, Ramakrishna V, *et al.* Evidence that an OX-2-positive cell can inhibit the stimulation of type 1 cytokine production by bone marrow-derived B7-1 (and B7-2)-positive dendritic cells. *Journal of Immunology*. 1999; 162: 774–781.

- [18] Coles SJ, Gilmour MN, Reid R, Knapper S, Burnett AK, Man S, *et al.* The immunosuppressive ligands PD-L1 and CD200 are linked in AML T-cell immunosuppression: identification of a new immunotherapeutic synapse. *Leukemia*. 2015; 29: 1952–1954.
- [19] Siva A, Xin H, Qin F, Oltean D, Bowdish KS, Kretz-Rommel A. Immune modulation by melanoma and ovarian tumor cells through expression of the immunosuppressive molecule CD200. *Cancer Immunology, Immunotherapy*. 2008; 57: 987–996.
- [20] Chen L, Huang X, Wang L, Wang C, Tang X, Gu M, *et al.* Electroacupuncture Reduces Oocyte Number and Maintains Vascular Barrier Against Ovarian Hyperstimulation Syndrome by Regulating CD200. *Frontiers in Cell and Developmental Biology*. 2021; 9: 648578.
- [21] Livak KJ, Schmittgen TD. Analysis of relative gene expression data using real-time quantitative PCR and the 2<sup>-ΔΔC<sub>T</sub></sup> Method. *Methods*. 2001; 25: 402–408.
- [22] Mashouri L, Yousefi H, Aref AR, Ahadi AM, Molaei F, Alahari SK. Exosomes: composition, biogenesis, and mechanisms in cancer metastasis and drug resistance. *Molecular Cancer*. 2019; 18: 75.
- [23] Fang Z, Jung KH, Yan HH, Kim SJ, Son MK, Rumman M, *et al.* CD-200 induces apoptosis and inhibits Bcr-Abl signaling in imatinib-resistant chronic myeloid leukemia with T315I mutation. *International Journal of Oncology*. 2015; 47: 253–261.
- [24] Jung YS, Vermeer PD, Vermeer DW, Lee SJ, Goh AR, Ahn HJ, *et al.* CD200: association with cancer stem cell features and response to chemoradiation in head and neck squamous cell carcinoma. *Head & Neck*. 2015; 37: 327–335.
- [25] Huotari J, Helenius A. Endosome maturation. *EMBO Journal*. 2011; 30: 3481–3500.
- [26] Kobayashi H, Tanaka N, Asao H, Miura S, Kyuuma M, Semura K, *et al.* Hrs, a mammalian master molecule in vesicular transport and protein sorting, suppresses the degradation of ESCRT proteins signal transducing adaptor molecule 1 and 2. *Journal of Biological Chemistry*. 2005; 280: 10468–10477.
- [27] D'Arena G, Vitale C, Coscia M, Lamorte D, Pietrantuono G, Perutelli F, *et al.* CD200 Baseline Serum Levels Predict Prognosis of Chronic Lymphocytic Leukemia. *Cancers*. 2021; 13: 4239.
- [28] Bhatt A, Bakrin N, Kammar P, Mehta S, Sinukumar S, Parikh L, *et al.* Distribution of residual disease in the peritoneum following neoadjuvant chemotherapy in advanced epithelial ovarian cancer and its potential therapeutic implications. *European Journal of Surgical Oncology*. 2021; 47: 181–187.
- [29] Takaya H, Nakai H, Sakai K, Nishio K, Murakami K, Mandai M, *et al.* Intratumor heterogeneity and homologous recombination deficiency of high-grade serous ovarian cancer are associated with prognosis and molecular subtype and change in treatment course. *Gynecologic Oncology*. 2020; 156: 415–422.
- [30] Wang Y, Li N, Ren Y, Zhao J. Association of BRCA1/2 mutations with prognosis and surgical cytoreduction outcomes in ovarian cancer patients: An updated meta-analysis. *Journal of Obstetrics and Gynaecology Research*. 2022; 48: 2270–2284.
- [31] Liu JQ, Hu A, Zhu J, Yu J, Talebian F, Bai XF. CD200-CD200R Pathway in the Regulation of Tumor Immune Microenvironment and Immunotherapy. *Advances in Experimental Medicine and Biology*. 2020; 1223: 155–165.
- [32] Mysona D, Pyrzak A, Purohit S, Zhi W, Sharma A, Tran L, *et al.* A combined score of clinical factors and serum proteins can predict time to recurrence in high grade serous ovarian cancer. *Gynecologic Oncology*. 2019; 152: 574–580.
- [33] Alegria-Baños JA, Jiménez-López JC, Vergara-Castañeda A, de León DFC, Mohar-Betancourt A, Pérez-Montiel D, *et al.* Kinetics of HE4 and CA125 as prognosis biomarkers during neoadjuvant chemotherapy in advanced epithelial ovarian cancer. *Journal of Ovarian Research*. 2021; 14: 96.
- [34] Rong Y, Li L. Early clearance of serum HE4 and CA125 in predicting platinum sensitivity and prognosis in epithelial ovarian cancer. *Journal of Ovarian Research*. 2021; 14: 2.